

**SYNTHESIS, MOLECULAR STRUCTURE AND SPECTROSCOPIC
AND COMPUTATIONAL STUDIES ON
4-(2-(2-(2-FORMYLPHENOXY)ETHOXY)ETHOXY)PHTHALONITRILE
AS A FUNCTIONALIZED PHTHALONITRILE**

Pınar Sen^{1*}, Salih Zeki Yıldız², Vildan Enisoglu Atalay³, Sibel Demir Kanmazalp^{4,5}, Necmi Dege⁶

¹Centre for Nanotechnology Innovation, Department of Chemistry, Rhodes University,
PO Box 94, Grahamstown, 6140, South Africa

²Sakarya University, Faculty of Arts and Sciences, Department of Chemistry,
54187 Sakarya, Turkey

³Uskudar University, Faculty of Engineering and Natural Sciences, Department of Bioengineering,
34662 Istanbul, Turkey

⁴Technical Sciences, Gaziantep University, Gaziantep, Turkey

⁵Physics Department, Gebze Technical University, Kocaeli, Turkey

⁶Ondokuz Mayıs University, Faculty of Arts and Sciences, Department of Physics,
55139 Samsun, Turkey

sen_pinar@hotmail.com

This work presents the synthesis and characterization of a novel compound, 4-(2-(2-(2-formylphenoxy)ethoxy)ethoxy)phthalonitrile as the aldehyde functional group substituted as a phthalonitrile derivative. The spectroscopic properties of the compound were examined through Fourier-transform infrared spectroscopy, Proton nuclear magnetic resonance, Carbon nuclear magnetic resonance, Ultraviolet-visible spectroscopy, Mass spectrometry and elemental analyses. The molecular structure of the compound was also confirmed using X-ray single-crystal data with a theoretical comparative approach.

Keywords: single crystal; aldehyde; phthalonitrile; DFT; HOMO; LUMO

**СИНТЕЗА, МОЛЕКУЛСКА СТРУКТУРА И СПЕКТРОСКОПСКА
И ПРЕСМЕТКОВНА СТУДИЈА
ЗА 4-(2-(2-(2-ФОРМИЛФЕНОКСИ)ЕТОКСИ)ЕТОКСИ)ФТАЛОНИТРИЛ
КАКО ФУНКЦИОНАЛИЗИРАН ФТАЛОНИТРИЛ**

Овој труд претставува синтеза и карактеризација на ново соединение, 4-(2-(2-(2-формилфенокси)етокси)етокси)фталонитрил како алдехидна функционална група супституирана како фталонитрилен дериват. Спектроскопските својства на соединението беа истражени со Фуриеова трансформна инфрацрвена спектроскопија, протонска нуклеарна магнетна резонанција, јаглеродна нуклеарна магнетна резонанција, ултравиолетова - видлива спектроскопија, масена спектрометрија и елементна анализа. Молекулската структура на соединението беше потврдена и со употреба на рендгенска дифракција на монокристал преку теоретски компаративен пристап.

Клучни зборови: монокристал; алдехид; фталонитрил; DFT; HOMO; LUMO

1. INTRODUCTION

Phthalonitrile derivatives are the most widely used precursors for the preparation of phthalocyanines, an important class of molecules [1]. In addition, phthalonitriles are used for the synthesis of high-performance polymers that display good mechanical properties and thermal stability [2].

A comprehensive understanding of phthalocyanine compounds continues to this day due to increasing interest on the 18- π electronic delocalization, thermal, photostability, coordination and optical properties. Their architectural flexibility also allows for the chemical and physical properties of these molecules to be regulated, which is an extraordinary feature for material science and allows these compounds to be used in many applications such as chemical sensors, photodynamic cancer therapy, liquid crystals, catalysis and non-linear optics [3–7].

The preparation of phthalocyanines is carried out via a cyclotetramerization reaction of phthalonitriles. The synthesis of phthalonitriles carrying functional groups leads to the formation of functionalized phthalocyanines. Phthalocyanines containing reactive groups have been a target of interest for chemists to switch to new molecular materials [8].

In this context, the development of aldehyde-substituted phthalocyanines from related phthalonitriles is crucial since they may carry out further chemical reactions on the macrocycle to prepare a Schiff base which is important for the development of coordination chemistry [9].

Using quantum chemistry and computation methodologies can elucidate atomic structures, charges and energetic information of the systems with an accuracy equivalent to or greater than those obtained experimentally. Therefore, theoretical calculations have been widely used as an effective tool for the intelligent design of new structures and for the investigation of the underlying structure-activity relationship.

In this study, the synthesis and characterization of 4-(2-(2-(2-formylphenoxy)ethoxy)ethoxy)phthalonitrile was performed to prepare an alternative starting material for the synthesis of different aldehyde substituted phthalocyanines. The x-ray crystallographic characterization of the second phthalonitrile derivative was performed as well as computational studies, which included geometry optimizations, HOMO and LUMO energies, determining molecular descriptors and NMR. These studies were performed with the DFT/B3LYP method in different solvents. The theoretical re-

sults obtained from the computational studies were compared with experimental data.

2. EXPERIMENTAL

2.1. Chemicals and instruments

The following chemicals were obtained from Sigma-Aldrich; salicylaldehyde, 2-(2-chloroethoxy)ethanol, acetonitrile, K_2CO_3 , nitrophenylphthalonitrile, dimethylformamide (DMF), hexane, chloroform ($CHCl_3$), methanol (MeOH), ethanol (EtOH) and diethylether. All other reagents and solvents were reagent grade quality and obtained from commercial suppliers. All solvents were stored over molecular sieves (4Å) and subsequently dried and purified, as described by Perrin and Armarego [10]. An anaerobic, inert atmosphere was supplied by argon through a dual-bank vacuum-gas manifold system. Thin-Layer chromatography (TLC) was performed using silica gel 60-HF254 as an adsorbent. Column chromatography was performed with a silica gel (Merck grade 60) and size exclusion chromatography was conducted with a Bio-beads gel (SX-1). Melting points were determined using a Barnstad-Electrotermel 9200 apparatus and are uncorrected. Electronic spectra were recorded on a Shimadzu UV-2600 Pc-spectrophotometer with a 1 cm quartz cell. Infrared spectra were recorded on a Perkin Elmer Spectrum two FT-IR spectrophotometer equipped with Perkin Elmer UATR-TWO diamond ATR and corrected by applying the ATR-correction function of Perkin Elmer Spectrum software. The 1H and ^{13}C NMR spectra were recorded with a Varian Mercury Plus 300 MHz spectrometer. Mass analysis was measured on a Micro-Mass Quatro LC/ULTIMA LC-MS/MS spectrometer. The elemental composition of the sample was analyzed with an element analyser (Flash 2000, Thermo Scientific).

2.2. X-ray crystallography

A suitable single crystal of the title compound was mounted on goniometer and data were collected at a STOE IPDS II (2 image plate detector) using a graphite monochromated $MoK\alpha$ radiation ($\lambda = 0.71073 \text{ \AA}$). Cell parameters of the compound were determined with WinGX software [11]. The structure of the titled compound was solved by the direct methods procedure in the SHELXS-97 program [12]; all the non-hydrogen atoms were refined anisotropically using the SHELXL-2014/7 program [13].

The molecular figures were prepared with the help of Mercury and ORTEP-3 program packages [14, 15]. All geometrical calculations were carried out using the program PLATON [16]. All non-hydrogen atoms were fixed geometrically. Selected crystallographic and refinement results for the compound are presented in Table 1.

CCDC 1585050 contains supplementary crystallographic data (excluding structure factors)

for the compounds reported in this article. These data can be obtained free of charge via <http://www.ccdc.cam.ac.uk/deposit> [or from the Cambridge Crystallographic Data Centre (CCDC), 12 Union Road, Cambridge CB2 1EZ, UK; fax: +44(0)1223 336033; e-mail: deposit@ccdc.cam.ac.uk].

Table 1

Crystallographic data and refinement parameters for the compound, C₁₈H₁₈C₁₄N₄O₄S₂

Crystal data	
Chemical formula	C ₁₉ H ₁₆ N ₂ O ₄
Mr	336.34
Crystal system, space group	Monoclinic, <i>P</i> 2 ₁ / <i>c</i>
Temperature (K)	296
a, b, c (Å)	13.6125 (12), 15.9430 (15), 8.4237 (7)
β (°)	107.059 (6)
V (Å ³)	1747.7 (3)
Z	4
Radiation type	Mo <i>K</i> α
μ (mm ⁻¹)	0.09
Crystal size (mm)	0.75 × 0.32 × 0.09
Data collection	
Diffractometer	STOE <i>IPDS</i> 2 diffractometer
Absorption correction	Integration
Tmin, Tmax	0.600, 0.790
No. of measured, independent and observed [<i>I</i> > 2 σ (<i>I</i>)] reflections	13779, 3252, 1352
Rint	0.129
(sin θ / λ) _{max} (Å ⁻¹)	0.606
Refinement	
$R[F^2 > 2\sigma(F^2)]$, $wR(F^2)$, <i>S</i>	0.085, 0.195, 1.01
H-atom treatment	H-atom parameters constrained
$\Delta\rho_{\text{max}}$, $\Delta\rho_{\text{min}}$ (e Å ⁻³)	0.18, -0.19

2.3. Computational methods

A conformational search to determine the stable structure of synthesized compound was performed with a semi-empirical PM6 method [17] using the program Spartan'16 v1.1.4 [18]. The obtained most stable conformer structure was optimized with a semi-empirical PM6 method and the Density Functional Theory (DFT) B3LYP (Becke's Three Parameter Hybrid Functional using the Lee, Yang and Parr Correlation Functional) [19] with the 6-311++G(d,p) method in the gas and DMF phases with the IEF-PCM approach [20]. The E_{HOMO} - E_{LUMO} were calculated using time-dependent

density functional theory (TD-DFT) at the B3LYP/6-311+G(d,p) levels in DMF phase, which was done by using the Self-Consistent Reaction Field (SCRF) method. The calculation of nuclear magnetic resonance (NMR) shielding tensors with the Gauge-Independent Atomic Orbital (GIAO) [21] method was computed with same basis set for the synthesized compound when gas, CDCl₃ or d-DMSO were used as a solvent. At the same time molecular descriptors such as electronegativity (χ), electron affinity (*A*), hardness (η), softness (*S*), electrophilicity index (ω) must be defined by the same computational methods. There is a practical calculation method to calculate for chemical hard-

ness (η) and electronegativity (χ) (Eq. 1), as given by Parr and Pearson [22].

$$\eta \approx \frac{I-A}{2}, \quad \chi \approx \frac{I+A}{2} \quad \text{Eq. 1}$$

where I is the ionization potential and A is the electron affinity. The Koopman's theorem was used for the calculation of I and A values derived from the frontier orbital energies of optimized neutral molecules, according to this theorem $I = -E_{\text{HOMO}}$ and $A = -E_{\text{LUMO}}$. Using Koopman's theorem, the chemical hardness and electronegativity are defined in terms of orbital energies (Eq. 2):

$$\eta \approx \frac{E(\text{LUMO}) - E(\text{HOMO})}{2},$$

$$x = -\mu \approx \frac{-E(\text{LUMO}) - E(\text{HOMO})}{2} \quad \text{Eq. 2}$$

The ω and S values are calculated by the following Eq. 3:

$$\omega \approx \mu^2/2\eta, \quad S \approx \frac{1}{(2\eta)} \quad \text{Eq. 3}$$

All visualizations and calculations were carried out with the methods implemented in GaussView5.0 [23] and Gaussian 09 package [24].

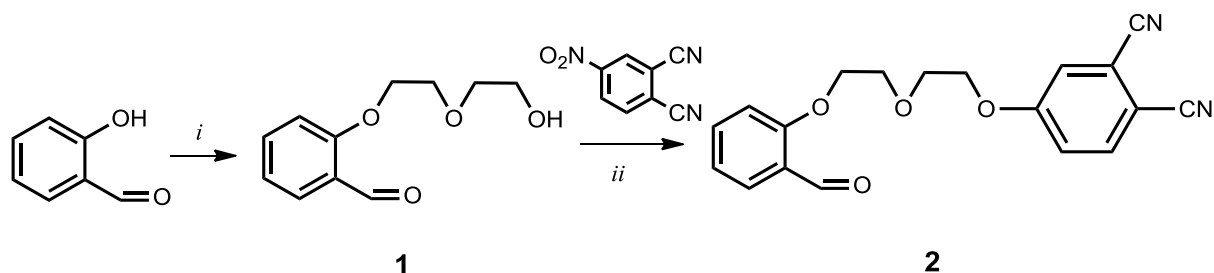
2.4. Synthesis

2.4.1. 2-(2-(2-hydroxyethoxy)ethoxy)benzaldehyde (**1**)

The preparation of **1** was carried out by reaction of salicylaldehyde and 2-(2-chloroethoxy)ethanol according to the published literature [25]. The spectral data of **1** are in accordance with the published structure.

2.4.2. 4-(2-(2-(2-formylphenoxy)ethoxy)ethoxy)phthalonitrile (**2**)

4-Nitrophthalonitrile (0.5 g, 2.9 mmol) and 2-(2-(2-hydroxyethoxy)ethoxy)benzaldehyde (**1**)



Scheme 1. Synthesis route: (i) 2-(2-chloroethoxy)ethanol, K_2CO_3 , (**1**), CH_3CN , reflux (ii) DMF, K_2CO_3 , 4-nitrophthalonitrile, 60°C

(0.61 g; 2.9 mmol) were dissolved in N,N- dimethylformamide (15ml), dissolved and degassed by argon in a dual-bank vacuum-gas manifold system. After stirring for 15 minutes, finely ground anhydrous potassium carbonate (1 g, 7.2 mmol) was added portion-wise over two hours with efficient stirring. The suspension solution was maintained at 60°C for 24 hours. The progress of the reaction was monitored by TLC using $\text{CHCl}_3/\text{Hexane}$ (5/1) solvent system. When the reaction was completed, the crude product was precipitated by pouring it into ice water (100 ml). The water phase was extracted with diethylether (3×25 ml) and the combined organic extracts were washed with water and dried over Na_2SO_4 . The product was then purified with column chromatography on a silica-gel and eluting with a $\text{CHCl}_3/\text{Hexane}$ (5/1) solvent system to yield (**2**) as white solid (yield = 92 % (0.89 g)). FT-IR (UATR-TWOTM) ν max/ cm^{-1} : 3078 (Ar, C-H), 2935-2873 (Aliph., C-H), 2720 (O=C-H), 2229 ($\text{C}\equiv\text{N}$), 1681 ($\text{C}=\text{O}$), 1597 (C=C), 1485,1454 (C-C), 1286 (Asym., Ar-O-), 1242 (C-O-C), 1161 (Sym., Ar-O-), 1134, 1097, 1043, 831, 759. ¹H-NMR (DMSO) δ (ppm): 10.34 (s, 1H), 8.24 (d, 1H), 8.01–8.06 (m, 2H), 7.74–7.66 (m, 1H), 7.45 (d, 1H), 7.23 (d, 1H), 7.05–7.11 (m, 1H), 4.30 (t, 4H), 3.88 (t, 4H). ¹³C-NMR (CDCl_3) δ (ppm): 190.64, 162.51, 159.12, 137.28, 128.12, 125.44, 124.99, 121.57, 120.92, 120.75, 117.78, 116.91, 116.42, 114.62, 111.27, 69.41, 68.96. MS (ESI): m/z 338.25 $[\text{M}+1]^+$, 372.23 $[\text{M}+2\text{H}_2\text{O}]^+$, 322.23 $[\text{M}-\text{CHO}]^+$

Anal. Calc. for $\text{C}_{19}\text{H}_{16}\text{N}_2\text{O}_4$ (%): C, 67.85; H, 4.79; N, 8.33; O, 19.03; Found (%): C, 67.68; H, 4.81; N, 8.30.

3. RESULTS AND DISCUSSION

3.1. Synthesis and spectroscopic characterization

Scheme 1 shows the synthetic route for target compound **2**.

As a first step, 2-(2-(2-hydroxyethoxy)ethoxy)benzaldehyde (**1**) was prepared by reacting of commercially available salicylaldehyde with 2-(2-chloroethoxy)ethanol in acetonitrile in the presence of K_2CO_3 using an established procedure [25]. The compound 4-(2-(2-(2-formylphenoxy)ethoxy)ethoxy)phthalonitrile (**2**) was obtained as a white powder from the reaction of 2-(2-(2-hydroxyethoxy)ethoxy)benzaldehyde (**1**) and 4-nitro-phthalonitrile, using K_2CO_3 as a catalyst in DMF through stirring at 60 °C for 24 hours. The purification of **2** was performed by column chromatography (silica gel, eluent: $CHCl_3$ /Hexane – 5/1), resulting in 92 % yield. A suitable crystal of molecule **2** was isolated for x-ray analysis upon crystallization from a $CHCl_3$ /methanol solution.

The characterization of product (**2**) was carried out through combination of methods in-

cluding FT-IR, 1H -NMR, ^{13}C -NMR, mass spectroscopy and elemental analysis. All the spectral data are in accordance with the proposed structure. More specifically, when comparing the FT-IR spectra of **1** and **2**, the disappearance of $-OH$ vibration at 3399 cm^{-1} and the appearance of new absorption bands at 2229 cm^{-1} clearly indicated the formation of **2**. The peak attributed to the $-C=O$ stretching was observed at 1657 cm^{-1} in the FT-IR spectra of compound **1**, but shifted to 1681 cm^{-1} in the FT-IR spectrum of compound **2**. In addition, the typical aliphatic $-C-H$ vibrational bands at $2935\text{--}2873\text{ cm}^{-1}$ were assigned to $-C-H$ stretching of the ethylene groups of compound **2**. The other sharp peaks at 1286 cm^{-1} , 1242 cm^{-1} , 1161 cm^{-1} and 1134 cm^{-1} were attributed to asym. Ar-O-, C-O-C, sym. Ar-O- and sym. Ar-O- stretching bands, respectively (Fig. 1).

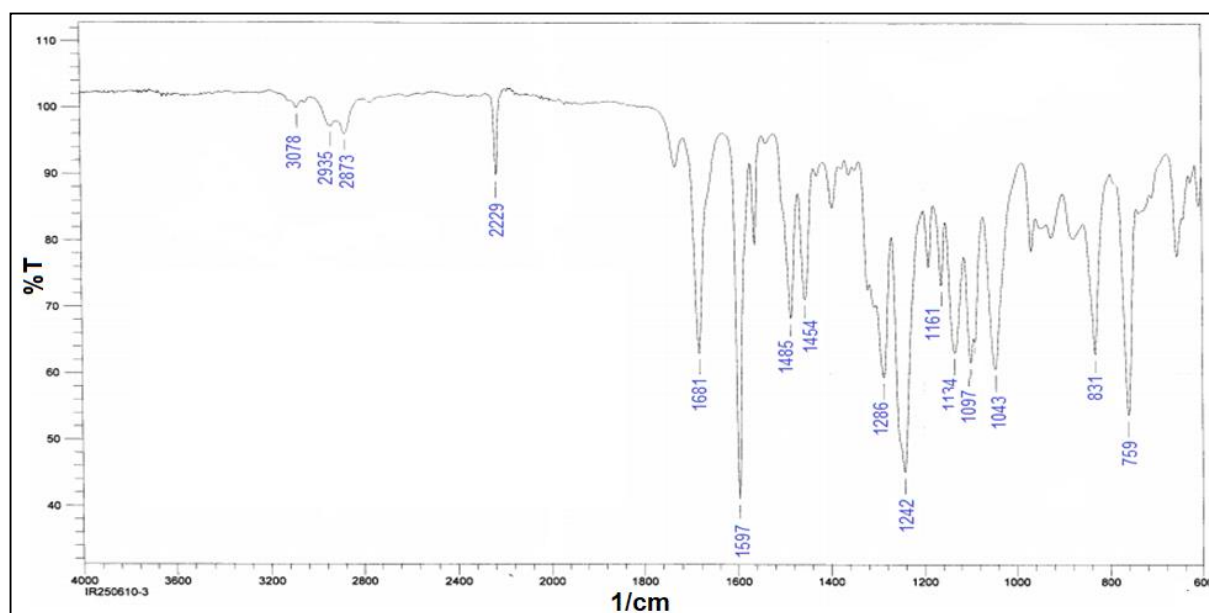


Figure 1. FT-IR spectrum of compound **2**

The 1H -NMR data provided satisfactory information about the proposed structure of the target compound (**2**). When comparing the 1H -NMR spectra of compound **1** and **2**, the disappearances of the OH proton signal of 2-(2-(2-hydroxyethoxy)ethoxy)benzaldehyde (**1**) in the 1H -NMR spectra in compound **2** and the appearance of new peaks in aromatic region at 8.24 ppm, 7.45 ppm, 7.23 ppm arising from phthalonitrile unit are evidence of the substitution of the phthalonitrile derivative **2** (Fig. 2). Aliphatic peaks belonging to ethylene chains were observed at 4.30 ppm and 3.88 ppm as a triplet; these peaks were expected results. The other aromatic peaks where the alde-

hyde is present were seen at 7.74–7.66 ppm, 7.45 ppm and 7.11–7.05 ppm. The characteristic aldehyde proton was detected as a singlet at 10.34 ppm.

In the ^{13}C -NMR spectrum of compound **2** (Fig. 3), the presence of the signal at 116.91 ppm and 116.42 ppm attributed to the nitrile carbon atoms are distinct differences from compound **1**. The aromatic carbon atoms peaks were appeared at between 162.51 ppm and 114.62 ppm. The aliphatic carbon peaks linking two aromatic rings emerged at 69.41 ppm and 68.96 ppm. The theoretical 1H and ^{13}C chemical shift values of the title compound are comparative with the experimental ones (Table 2).

The mass spectrum of compound **2** was obtained by the LC–MS/MS spectrometer, thus confirming the proposed structure. In the mass spectrum of **2**, the presence of molecular ion peak (m/z : 338.25 $[M+1]^+$) indicates the formation of desired product. Apart from the 2 moles of H_2O , there was an adducted ion peak at m/z : 372.23 $[M+2H_2O]^+$ and the fragment ion peak at 322.23 $[M-CHO]^+$ in the mass spectrum (Fig. 4)

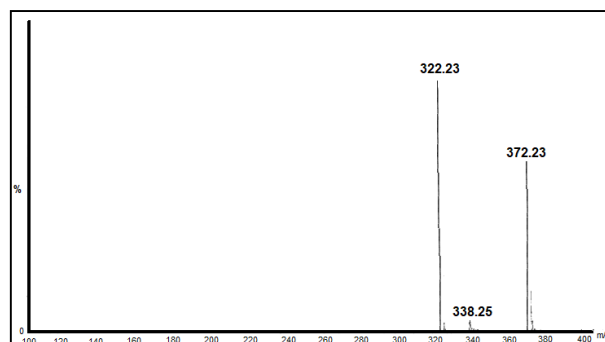


Figure 4. Mass spectrum of **2**.

Table 2

Theoretical (according to the calculations of B3LYP/6-311+G(d,p) in different solvents) and experimental ^{13}C and 1H isotropic chemical shifts with respect to TMS. All values are given in ppm.

	Atom number	In gas	In d-DMSO	In $CDCl_3$	Experimental
^{13}C	C19	195.357	198.3438	198.8295	190.64
	C4	172.7184	174.6568	175.0534	162.51
	C13	171.5166	173.067	173.4391	159.12
	C6	127.2665	129.3075	129.7005	137.28
	C15	145.2828	147.1157	147.4991	128.12
	C17	138.538	138.0221	138.1751	125.44
	C18	133.2326	133.5225	133.7743	124.99
	C16	129.4018	129.2806	129.5107	121.57
	C5	130.3418	132.3476	132.7441	120.92
	C3	144.8431	146.0819	146.4103	120.75
	C2	117.5702	115.5764	115.6195	117.78
	C1	123.4168	126.3592	126.8614	116.91
	C8	124.0669	126.4402	126.8804	116.42
	C14	116.9981	118.9701	119.3954	114.62
	C7	126.8688	126.022	126.1841	111.27
	C10	79.945	80.244	80.504	69.41
C11	77.845	78.032	78.279	69.41	
C9	75.141	76.207	76.529	68.96	
C12	73.092	74.12	74.445	68.96	
1H	s, 1H; H19	11.16	11.1326	11.1321	10.34
	d, 1H; H6	8.2259	8.3852	8.40	8.24
	s, 1H; H3	8.3009	8.5082	8.5277	8.07
	d, 1H; H17	8.8364	8.7732	8.7681	8.01
	m, 1H; H15	8.3119	8.465	8.4809	7.74
	m, 1H; H5	7.8965	8.0819	8.099	7.45
	d, 1H; H14	7.4251	7.6498	7.6744	7.23
	t, 1H; H16	7.8211	7.8667	7.8717	7.05
	t, 2H; H12	4.9296	4.9517	4.9561	4.3
	t, 2H; H9	4.9217	5.1713	5.0827	4.3
	t, 2H; H11	4.5015	4.563	4.5693	3.88
t, 2H; H10	4.5296	4.6735	4.6894	3.88	

3.2. Crystal structure description of the compound

The compound crystallizes in the monoclinic space group $P2_1/c$ with one molecule in the asymmetric unit. The single crystal X-ray structure is shown in Figure 5. In the title compound, the phthalonitrile ring and the formylphenoxy ring are non-planar, while the dihedral angle between the two rings is $79.4(1)^\circ$.

The selected geometric parameters (Table 3) at oxygen and nitrogen atoms also show substantial variations from threefold symmetry. The similarity of the C—O bond lengths, apart from the C19—O4 bond length, indicates localized bonding arrangements rather than delocalized bonds. The O4—C19—C18 angle around the carbonyl carbon of the aldehyde group is $122.5(6)^\circ$. At the same time, this angle was calculated with the theoretical method, which reported the O—C—C angle as

124.886° and -124.906° in gas and DMF phases, respectively.

The conformation about the two cyano groups C1—N1 and C8—N2 bonds are $1.141(6)$ and $1.140(7)$ Å (where the N1—C1—C2 and N2—C8—C7 dihedral angle is $179.0(6)$ and $178.4(6)^\circ$, respectively (Table 3). These lengths follow literature values [26]. The optimized geometric structure with DFT/B3LYP/6-311++G(d,p) method in the gas and DMF phases is also compared with the experimental values in Table 3. These C1—N1 and C8—N2 bonds lengths are computed 1.15505 and 1.15561 Å in gas and 1.5523 and 1.15621 Å in DMF phase, respectively. Furthermore, the N1—C1—C2 and N2—C8—C7 dihedral angles are calculated 177.890 and 178.628° in gas and 178.939 and 179.101° in DMF phase, respectively. The obtained values in the solvent phase overlap more according to the gas phase.

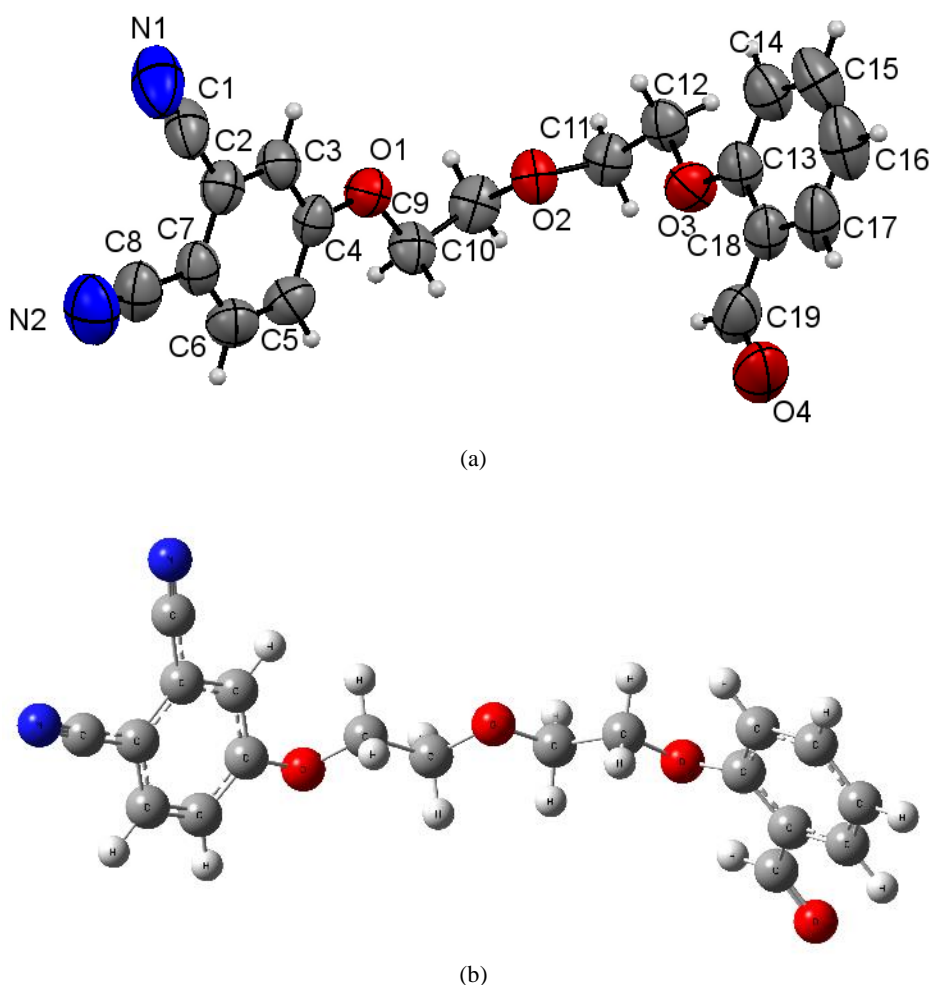


Figure 5. (a) The molecular structure of the C₁₉H₁₆N₂O₄ with the displacement ellipsoids of non-hydrogen atoms drawn at the 30 % probability level. (b) Optimized structure of the title compound

Table 3

Selected bond lengths (Å) and angles (°) for $C_{19}H_{16}N_2O_4$ structure. These data include those obtained experimentally and those calculated with the DFT/B3LYP/6-311++G(d,p) method in both gas and DMF phases

	Exp	Calculated	
		In gas	In DMF
Bond lengths (Å)			
O2—C10	1.414 (5)	1.41523	1.41824
O2—C11	1.416 (5)	1.41931	1.42122
O1—C4	1.346 (5)	1.35697	1.35117
O1—C9	1.432 (5)	1.43439	1.44090
O3—C13	1.352 (6)	1.36243	1.35733
O3—C12	1.426 (5)	1.42580	1.43249
O4—C19	1.226 (6)	1.21533	1.22016
C1—N1	1.141 (6)	1.15505	1.5523
C8—N2	1.140 (7)	1.15561	1.15621
Bond angles (°)			
C10—O2—C11	112.1 (3)	114.548	113.519
C4—O1—C9	119.3 (4)	121.749	119.635
C13—O3—C12	119.4 (4)	119.867	119.742
O1—C4—C3	116.3 (5)	124.886	124.906
N1—C1—C2	179.0 (6)	177.890	178.939
N2—C8—C7	178.4 (6)	178.628	179.101
O4—C19—C18	122.5 (6)	124.886	124.906
Torsion angles (°)			
C4—O1—C9—C10	-173.2 (4)	96.523	97.656
C12—O3—C13—C14	1.2 (7)	-4.198	-1.24
O3—C12—C11—O2	71.9 (5)	72.452	71.732
O1—C9—C10—O2	68.9 (5)	71.750	70.756
C10—O2—C11—C12	175.3 (4)	165.865	170.314
C13—C18—C19—O4	176.3 (5)	179.696	179.329

In the crystal, hydrogen-bonding and Van der-Waals interactions are dominant. The H atoms in the phthalonitrile ring form intermolecular C—H...N and C—H...O interactions, linking molecules to form chains (Figure 6b). Intermolecular C—H... π interactions support hydrogen bond geometry. An interaction occurred between the centre of the Cg(2) ring identified with C13-C18 and the

H12a atom bonded to the C12 atom [C12—H12a...Cg(2)ⁱⁱⁱ; symmetry code; (iii) x,1/2-y,1/2+z]. Furthermore, the π - π stacking interactions between the phthalonitrile rings with a centroid-centroid [Cg(1)—Cg(1)] distance of 3.592 Å [Cg(1) are the centroid of the C2—C7 ring (symmetry code: -x,1-y,1-z)]. The detailed geometric parameters of the hydrogen bonds are given in Table 4.

Table 4

Hydrogen-bond geometries (Å, °) for $C_{19}H_{16}N_2O_4$

	D—H...A	D—H	H...A	D...A	D—H...A
C19—H19...O3		0.93	2.42	2.740(7)	100
C3—H3...O4 ⁱ		0.93	2.454	3.336	158
C5—H5...N1 ⁱⁱ		0.93	2.586	3.348	140
C12—H12a...Cg(2) ⁱⁱⁱ		0.97	2.75	3.56	142
Symmetry codes: i: x, -y+3/2, z-1/2; ii: -x+2, y+1/2, -z+3/2; iii: x,1/2-y,1/2+z; Cg(1):C2-C7.					

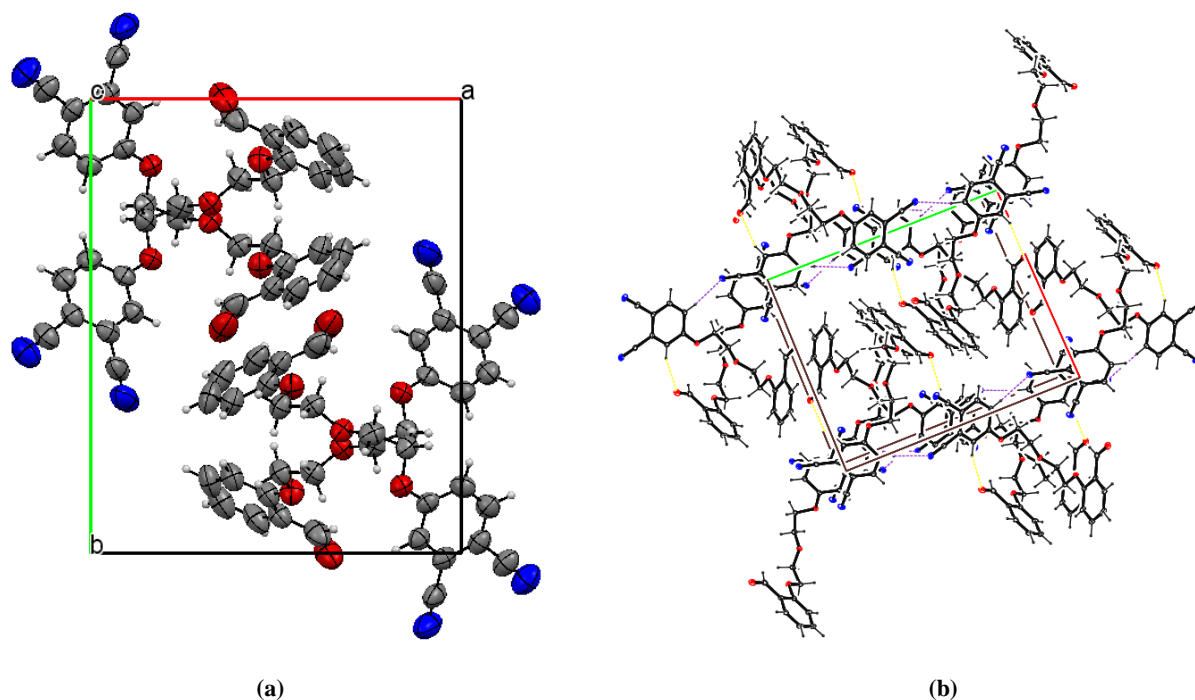


Figure 6. (a) Crystal-packing diagram of the title compound, $C_{19}H_{16}N_2O_4$, along the c -axis. (b) In the crystal-packing diagram, hydrogen bonds are shown as dashed lines along with $C5-H5\cdots N1$ (purple) and $C3-H3\cdots O4$ (yellow).

The HOMO-LUMO energies are directly related to ionization potential and electron affinity. The energy and distribution of the HOMO-LUMO orbitals and difference between $E_{HOMO}-E_{LUMO}$ gap are an essential point of stability for the molecules. A molecule with a small gap is more polarized and known as soft molecule. HOMO-LUMO orbital distribution and bandgap values of a synthesized compound were calculated by theoretical methods gathered in gas and DMF phases (Fig.7).

An important point that the HOMO orbitals are mainly localized on the formylphenoxy, whereas the LUMO orbitals are distributed within the phthalonitrile groups of the molecule. This means that the formylphenoxy group in the molecule would be more easily attacked. Another point is that $E_{HOMO}-E_{LUMO}$ bandgap (0.15926 eV) in DMSO is smallest value in all studied phases, showing that the molecule in the DMSO solvent has a stronger electron donating ability.

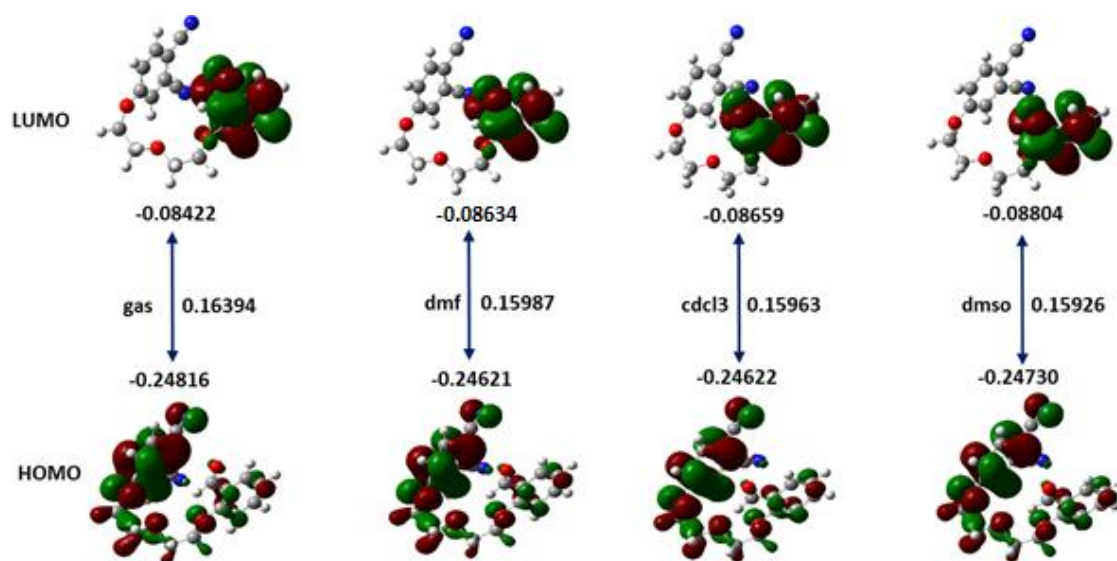


Figure 7. The HOMO-LUMO energies (eV) of the title molecule calculated by DFT/B3LYP/6-311+G(d,p) and bandgaps are in gas, DMF, DMSO and $CDCl_3$ phases

Molecular descriptor values obtained from the total energy for the title molecule in both gas and different solvents such as DMF, DMSO and CDCl_3 are listed in Table 5. The hardness value (η) is one-half the HOMO–LUMO gap of title molecule. Therefore, the larger the gap, the greater the hardness and thus stability of the title molecule. This property is therefore a powerful indicator that ultimately determines that hard molecules are less reactive than softer molecules. Table 5 shows that hardness is affected by solvent selectivity. In the gas phase and the phases of all of the studied solvents, the molecule has larger hardness value in when dissolved in DMSO. This finding is according to the

greater hardness value of the molecule, indicating its greater stability. As hard molecules are less reactive than softer molecules [27], the stability order is therefore $\text{DMSO} > \text{CDCl}_3 > \text{DMF} > \text{gas phase}$. A molecule with low chemical potential is a good electrophile, while an extremely hard molecule has feeble electron acceptability. Electrophilicity depends on both the chemical potential and the chemical hardness [28]. The calculated χ and ω values show that the more polar a solvent, the more it contributes to accentuate the parametric representation of activity. Additionally, we observed that solvent selection has a considerable effect on electrophile/nucleophile interactions.

Table 5

Molecular descriptors values of the title molecule calculated by DFT/B3LYP/6-311+G(d,p) level of theory

Molecular descriptors								
Solvent	E_{HOMO}	E_{LUMO}	A	I	η	χ	ω	S
Gas	-0.24816	-0.08422	0.24816	0.08422	-0.08197	0.16619	-0.16847	-6.09979
DMF	-0.24621	-0.08634	0.24621	0.08634	-0.07994	0.16628	-0.17294	-6.25508
DMSO	-0.24730	-0.08804	0.24730	0.08804	-0.07963	0.16767	-0.17652	-6.27904
CDCl_3	-0.24622	-0.08659	0.24622	0.08659	-0.07982	0.16641	-0.17347	-6.26449

4. CONCLUSION

In this work, 4-(2-(2-(2-formylphenoxy)ethoxy)ethoxy)phthalonitrile (compound **2**) was synthesized and characterized by FT-IR, ^1H -NMR, ^{13}C -NMR, UV-vis, MS, elemental analyses. This compound was obtained as single crystal, suitable for X-ray analysis. All crystallographic data agree with the theoretical bond lengths, angles, dihedral angles of compound **2**. The ^1H -NMR and ^{13}C -NMR results of the theoretical spectra agree with the experimental data. The value of the energy separation between the HOMO and LUMO provides important information about the title compound studied in gas, CDCl_3 and DMSO. The $E_{\text{HOMO}}-E_{\text{LUMO}}$ bandgap (0.15926 eV) in the DMSO is the smallest value in all studied phases, indicating that the molecule in DMSO solvent has stronger electron donating ability. Molecular descriptor values allow us to evaluate the molecule in terms of reactivity. These results imply that the molecule has larger hardness value in DMSO solvent, meaning that it is less reactive there than in any of the other studied solvents.

Acknowledgement. This work was supported by the Research Fund of Sakarya University (project no. 2014-02-04 007).

REFERENCES

- [1] W. M. Sharman, J. E. Lier, *The Porphyrin Handbook*, Academic Press, New York, 2003.
- [2] T. M. Keller, T. K. Price, Amine-cured bisphenol-linked phthalonitrile resins, *J. Macromol. Sci. Chem.* **18**, 931 (1982). DOI: <https://doi.org/10.1080/00222338208077208>
- [3] S. Radhakrishnann, S. D. Deshpande, Conducting polymers functionalized with phthalocyanine as nitrogen dioxide sensors, *Sensors*, **2**, 185–194 (2002). DOI: <https://doi.org/10.3390/s20500185>
- [4] R. Bonnett, *Chemical Aspects of Photodynamic Therapy*, Gordon and Breach Science, Canada, 2000.
- [5] M. Shimizu, L. Tauchi, T. Nakagaki, A. Ishikawa, E. Itoh, K. Ohta, Discotic liquid crystals of transition metal complexes 48: Synthesis of novel phthalocyanine-fullerene dyads and effect of a methoxy group on their clearing points, *J. Porphyrins Phthalocyanines*, **17**, 264–282 (2013). DOI: <https://doi.org/10.1142/S1088424613500752>
- [6] A. B. Sorokin, Phthalocyanine metal complexes in catalysis, *Chem. Rev.* **113**, 8152 (2013). DOI: 10.1021/cr4000072
- [7] G. Torre, P. Vazquez, F. Agullo-Lopez, T. Torres, Phthalocyanines and related compounds: organic targets

- for nonlinear optical applications, *J. Mater. Chem.* **8**, 1671–1683 (1998). DOI: 10.1039/A803533D
- [8] H. Kliesch, A. Weitemeyer, S. Miiller, D. Wohrle, Synthesis of phthalocyanines with one sulfonic acid, carboxylic acid, or amino group, *Liebigs Ann.* 1269–1273 (1995). DOI: <https://doi.org/10.1002/jlac.1995199507168>
- [9] P. Sen, S. Z. Yildiz, M. Tuna, M. Canlica, Preparation of aldehyde substituted phthalocyanines with improved yield and their use for Schiff base metal complex formation, *J. Organomet. Chem.*, **769**, 38–45 (2014). DOI: <https://doi.org/10.1016/j.jorganchem.2014.07.007>
- [10] D. D. Perrin, W. L. F. Armarego, D. R. Perrin, *Purification of Laboratory Chemicals*, Pergamon Press, New York (2013).
- [11] G. M. Sheldrick, A short history of SHELX, *Acta Cryst. A*, **64**, 112 (2008). DOI: <https://doi.org/10.1107/S0108767307043930>
- [12] G. M. Sheldrick, *SHELXS97 and SHELXL97*, University of Gottingen, Germany, 1997.
- [13] G. M. Sheldrick, Crystal structure refinement with SHELXL, *Acta Cryst. C*, **71**, 3–8. (2015). DOI: <https://doi.org/10.1107/S2053229614024218>
- [14] C. F. Macrae, P. R. Edgington, P. McCabe, E. Pidcock, G. P. Shields, R. Taylor, M. Towler, J. Streek, Mercury: visualization and analysis of crystal structures, *J. Appl. Cryst.* **39**, 453 (2006). DOI: <https://doi.org/10.1107/S002188980600731X>
- [15] L. J. Farrugia, ORTEP-3 for Windows—a version of ORTEP-III with a Graphical User Interface (GUI), *J. Appl. Cryst.* **30**, 565 (1997). DOI: <https://doi.org/10.1107/S0021889897003117>
- [16] L. Spek, Single-crystal structure validation with the program PLATON, *J. Appl. Cryst.* **36**, 7 (2003). DOI: <https://doi.org/10.1107/S0021889802022112>
- [17] (a) J. J. P. Stewart, Application of the PM6 method to modeling the solid state, *J. Mol. Model.* **14**, 499–535 (2008). DOI: 10.1007/s00894-008-0299-7
(b) J. J. P. Stewart, Application of the PM6 method to modeling proteins, *J. Mol. Model.* **15**, 765–805 (2009). DOI: 10.1007/s00894-008-0420-y
- [18] Spartan'16 Wavefunction, Inc. Irvine, CA.
- [19] C. Lee, W. Yang, R. G. Parr, Development of the Colle-Salvetti correlation-energy formula into a functional of the electron density, *Phys. Rev. B*, **37**, 785 (1988). DOI: <https://doi.org/10.1103/PhysRevB.37.785>
- [20] G Scalmani, M. J. Frisch, Continuous surface charge polarizable continuum models of salvation. I. General formalism, *J. Chem. Phys.* **132**, 114110 (2010). DOI: <https://doi.org/10.1063/1.3359469>
- [21] (a) F. London, Théorie quantique des courants interatomiques dans les combinaisons aromatiques, *J. Phys. Radium*, **8**, 397–409 (1937). DOI: 10.1051/jphysrad:01937008010039700;
(b) J. R. Cheeseman, G. W. Trucks, T. A. Keith, M. J. Frisch, A comparison of models for calculating nuclear magnetic resonance shielding tensors, *J. Chem. Phys.* **104**, 5497–509 (1996). DOI: <https://doi.org/10.1063/1.471789>
- [22] (a) R. G. Parr, R. G. Pearson, Absolute hardness: companion parameter to absolute electronegativity, *J. Am. Chem. Soc.* **105**, 7512 (1983). DOI: 0002-7863/83/1505-7512\$01.50/0
(b) R.G. Pearson, Chemical hardness and bond dissociation energies, *J. Am. Chem. Soc.* **110**, 7684 (1988). DOI: 0002-7863/88/1510-7684\$01.50/0
- [23] R. Dennington, T. Keith, J. Millam, *GaussView, Version 5*, Semichem Inc., Shawnee Mission KS, 2009.
- [24] M. J. Frisch, G. W. Trucks, H. B. Schlegel, G. E. Scuseria, M. A. Robb, J. R. Cheeseman, J. A. Montgomery, J. T. Vreven, K. N. J. C. Kudin, J. M. Millam, S. S. Iyengar, J. Tomasi, V. Barone, B. Mennucci, M. Cossi, G. Scalmani, N. Rega, G. A. Petersson, H. Nakatsuji, M. Hada, M. Ehara, K. Toyota, R. Fukuda, J. Hasegawa, M. Ishida, T. Nakajima, Y. Honda, O. Kitao, H. Nakai, M. Klene, X. Li, J. E. Knox, H. P. Hratchian, J. B. Cross, C. Adamo, J. Jaramillo, R. Gomperts, R. E. Stratmann, O. Yazyev, A. J. Austin, R. Cammi, C. Pomelli, J. W. Ochterski, P. Y. Ayala, K. Morokuma, G. A. Voth, P. Salvador, J. J. Dannenberg, V. G. Zakrzewski, A. D. Daniels, O. Farkas, A. D. Rabuck, K. Raghavachari, J. V. Ortiz “*Gaussian 09*”, *Gaussian, Inc.*, Pittsburgh PA, 2009.
- [25] S. Wenger, Z. Asfari, J. Vicens, Synthesis of two calix[4]arenes constrained to a 1,3-alternate conformation by diaza-benzo crown ether bridging, *Tetrahedron Lett.* **35**, 8369–8372 (1994). DOI: [https://doi.org/10.1016/S0040-4039\(00\)74409-1](https://doi.org/10.1016/S0040-4039(00)74409-1)
- [26] P. Sen, G. Y. Atmaca, A. Erdogmus, S. D. Kanmazalp, N. Dege, S. Z. Yildiz, Peripherally tetra-benzimidazole units-substituted zinc(II) phthalocyanines: Synthesis, characterization and investigation of photophysical and photochemical properties, *J. Lumin.* **194**, 123–130 (2018). DOI: <https://doi.org/10.1016/j.jlumin.2017.10.022>
- [27] C. Fierro, A. B. Anderson, D. A. Scherson, Electron donor-acceptor properties of porphyrins, phthalocyanines, and related ring chelates: A molecular orbital approach, *J. Phys. Chem.* **92**, 6902–6907 (1988). DOI: 0022-3654/88/2092-6902\$01.50/0
- [28] N. Islam, D. C. Ghosh, On the electrophilic character of molecules through its relation with electronegativity and chemical hardness, *Int. J. Mol. Sci.* **13**, 2160–2175 (2012). DOI: <https://doi.org/10.3390/ijms13022160>